



## Fabrication of prototype connecting rod of PLA plastic material using FDM prototype technology

Nagendra Kumar Maurya<sup>a,b\*</sup>, Vikas Rastogi<sup>b</sup>, Pushpendra Singh<sup>b</sup>

<sup>a</sup>Department of Mechanical Engineering, G.L Bajaj Institute of Technology & Management, Greater Noida 201310, India

<sup>b</sup>Department of Mechanical Engineering, Delhi Technological University, New Delhi 110 042, India

*Received: 12 November 2018; Accepted: 11 March 2020*

Rapid prototyping (RP) have been attracting attention in the manufacturing community because of their capability to reduce the lead time of product development. Present work is an effort to understand the influence of process variables like infill pattern, layer thickness, build orientation and infill density on dimensional accuracy (DA), flatness and cylindricity. Taguchi method orthogonal array  $L_9$  was used for the conduction of experiments. MakerBot Replicator-2 was used for the fabrication of scaled prototype connecting rod of polylactic acid (PLA) material. DA, flatness and cylindricity of the component were measured by using coordinate measuring machine (CMM). Analysis of variance (ANOVA) was employed to find out the significance of process parameters. A regression model was developed to predict the DA, flatness and cylindricity. The results reveal that the optimum process parameters for the DA, flatness and cylindricity were different. Utility Theory was used to find out the best process parameter condition. The best process parameters for the DA, flatness and cylindricity was found to be layer thickness 100  $\mu\text{m}$ , linear infill pattern, inclined at 45° orientation and 20% infill density. A confirmation test was conducted for checking the goodness of the model, which reveals that results were within the confidence limit.

**Keywords:** Analysis of variance, Fused deposition modelling, Signal to noise (S/N) ratio, Taguchi method, Multi objective optimization

### 1 Introduction

Prototypes are most important for the conceptualization of design, manufacturing and analysis. RP are commonly used for the reduction of lead time at various stages of the product development cycle<sup>1-3</sup>. Making a prototype model is one of the key steps in the development of new product. Rapid prototyping has become a solution for making the prototype models globally. RP is an innovation in which components are generate in layer by layer arrangement. It is one of the fastest growing technologies by which prototypes model of any component can be built in just a few hours from 3D CAD design. Complexity of shape is not an issue in the RP process<sup>4-5</sup>. Nowadays, several rapid prototyping technologies are commercially available<sup>6</sup>. RP technology has a limitation that presently most of the available materials are not suitable with AM technology. This can be overcome by evolution of new materials or adjusting the process parameters while fabrication to get good accuracy<sup>7</sup>. Part orientation, layer thickness, infill pattern, infill

density, raster angle, shell density, air gap etc. are the main process parameters, which influence the dimensional accuracy of the parts manufactured by FDM<sup>8</sup>. MakerBot Replicator-2 is a 3D desktop printer in which complicated 3D parts can be generated layer upon layer. CAD model is sliced into layers of 0.1 to 0.4 mm height. The acrylonitrile butadiene styrene (ABS) and poly lactic acid (PLA) material are generally used in FDM process. FDM wires are extruded through extrusion nozzle. MakerBot print software specified to deposit the material of specific layer thickness by controlling the position of nozzle<sup>9</sup>. The geometrical tolerance in part printed through AM mostly depends on the effective use of the process parameters<sup>10-11</sup>.

Numerous attempts have been made to understand the effect of process parameter on DA, flatness and cylindricity optimization of FDM prototypes. Chang & Huang<sup>12</sup> have studied on profile error extruding aperture for the FDM process. The process parameters such as raster width, contour width, raster angle and contour depth are chosen for the optimization of flatness and cylindricity. From the ANOVA analysis of individual process variable it is concluded that

\*Corresponding author (E-mail:nagendramnit@gmail.com)

contour depth has highest contribution (38.20%). Contour width is the second dominating factor (28.73%), Raster width has (0.1%) and raster angle (7%) contribution. Das *et al.*<sup>13</sup> have worked on optimizing the part build orientation and developed a mathematical model between part orientations, geometric dimensioning & tolerances (GD & T) errors on the part printed by RP process. An algorithm was developed for the build orientation which minimizes the volume of the support material. Paul and Anand<sup>7</sup> have worked on the optimization of process variable for reducing form errors with less support structures. The analysis was focused on the impact of process variable i.e. orientation on flatness and cylindricity. Saqib and Urbanic<sup>14</sup> have carried out experimental studies on flatness, cylindricity and perpendicularity to identify and measure the influence of main process variables for the deformation of RP parts. The study was focused on the layer thickness, work envelop and orientation. The result reveals that variation in cylindricity was maximum at 90° orientations.

Mohame *et al.*<sup>15</sup> have used response surface methodology to select the correct parameters for reducing build time without compromising the quality of the product. ANOVA analysis was used to find the effect of individual parameters. Result of multi objective optimization reveal that the optimal process parameters conditions was air gap = 0.499 mm, layer thickness = 0.2540 mm, raster angle = 0.0000266, road width = 0.484 mm, orientation = 0.0000339° and number of couture 7.

Nitin *et al.*<sup>16</sup> have calculated circularity and surface finish of ABS part fabricated by FDM process using Taguchi method (L<sub>27</sub>) orthogonal array. The optimal setting for the process parameters for the surface roughness and circularity was bed temperature of 110 °C, print speed of 35mm/s, layer thickness of 0.4 mm, number of loops of 3, infill of 30 % and nozzle temperature of 220 °C. Das *et al.*<sup>17</sup> have studied on optimization for the flatness, cylindricity, parallelism and perpendicularity tolerances with build orientation which minimize the support contact area and support material. Aljohani and Desai<sup>18</sup> have conducted experimental investigation to find out the effect of infill pattern on mechanical properties and porosity in FDM component. Knoop and Schoeppner<sup>19</sup> have conducted experimental study to find out the effect of process parameters on geometrical accuracy of ABS material fabricated by FMD process. Holes and

cylinders of cylindrical element were investigated. The result shows that DA is better in the XY plane. Juneja *et al.*<sup>20</sup> have conducted experimental study to investigate the DA of surgical guides by using different 3D printing technology like polyjet, SLA and FDM. Results depict that the DA of component fabricated by RP was better than conventional methods.

Kozior *et al.*<sup>21</sup> have evaluated the effect of FDM process parameters on mechanical properties like Young's modulus and stress relaxation of ABS P430 material during uniaxial compression test. Effects of printing direction and orientation on mechanical properties were evaluated. Results of experimental study depicted that printing direction have significant effect on the mechanical properties. Young's modulus and modulus of elasticity were found to be maximum at 0° orientation. However, mechanical properties were found to be minimum at 45° orientation. Kozior *et al.*<sup>22</sup> have evaluated the effect of fabric pretreatment on adhesion of 3D printed material on textile substrates. Results show that pretreatment has significant effect on adhesion forces. It was also observed that adhesion phenomena are affected by infill orientation. Adhesion force was found to be maximum at 90° orientation. However, pretreatment has less impact on tensile strength and elongation at break. Surface roughness was found to be minimum at 0° infill orientation. Maurya *et al.*<sup>23</sup> have investigated the impact of reinforcement of high strength PETG material on ultimate tensile strength of ABS and PLA material. Results depicted that due to the reinforcement ultimate tensile strength of ABS material was improved about 70 % and ultimate tensile strength of PLA material was improved about 8%.

After literature survey, it was found that the effect of infill pattern was carried out to check the mechanical properties only. Infill pattern significantly affect the mechanical properties. It was also found that impact of infill pattern varied with the change of infill density and layer thickness. This research work was carried out to find out the impact of process variables viz infill pattern, layer thickness, infill density and orientation on DA and form error (flatness and cylindricity). Radial engine connecting rod was considered as a component. Coordinate measuring machine (CMM) was employed to measure the DA and form error in the selected component. The novelty of this work lie in the fact that no such study

have been carried out to investigate DA, flatness and cylindricity using these parameters for the PLA material in the archival literature. The emphasis of this study is to develop the relation between process variables such as layer thickness, orientation, infill pattern and infill density on DA, cylindricity and flatness. Utility Theory (multi objective optimization) is employed to find out the best process parameters condition for the DA, flatness and cylindricity.

**2 Material and Method**

**2.1 3D modelling and fabrication of component**

The aim of this study was to systematically measure the DA and form error present in the fabricated prototype component by FDM technology. A connecting rod of radial engine with scaled model was selected as specimen. Selected component have linear dimension, radial dimension, cylindrical as well as flat surface. For 3D modelling, standard modelling software CATIA V6 was used. CAD model was converted into STL file which is required for the all the 3D printing technology. Figure1 shows the 3D CAD model of the connecting rod. PLA plastic was used for build and support material in this study. In this work, experimental studies were carried out to investigate the impact of process parameters like layer thickness, infill pattern, orientation and infill density on DA, flatness and cylindricity at constant raster angle (45 degree). Taguchi orthogonal array (L<sub>9</sub>) was employed for the conduction of experiment. Components were fabricated by MakerBot Replicator-2, 3D desktop printer. Figure 2 shows the fabricated prototype component of the connecting rod. To ensure the repeatability of the result three specimens were fabricated for the each set of experiment and average value of each group were used for the analysis. Total

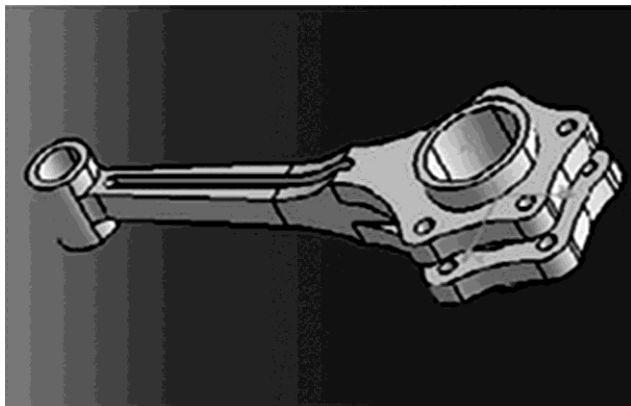


Fig.1 — 3D CAD model of connecting rod.

27 samples were fabricated, 3 samples for the each groups of experiment. The part orientation while fabrication was as shown in Fig. 3 (a, b & c). Types of infill pattern used in this work, is shown in Fig. 4. Table 1 illustrates the details of process parameters & their levels. The experimental plan for the each trial was reported in Table 2.

The component fabricated through FDM process contains support material on its surface, which is removed after the fabricated component. In the removal process, it creates burrs on the surface, if proper mechanism is not used. In this work, special designed hand tools were used for the removal of support material. However, when support material is not carefully removed from the surface of build material, some scratches formed on the surface which yields poor surface roughness and shape distortion. It



Fig. 2 — Physical model of connecting rod.

Table 1 — Process parameters & levels.

S.No.	Process parameters	Level1	Level 2	Level3
1	Layer thickness (µm)	100	200	300
2	Infill Pattern	Linear	Hexagonal	Moroccan Star fill
3	Orientation	Flat	Edge	Inclined at 45°
4	Infill density (%)	20	40	60

Table 2 — Taguchi’s L9 orthogonal array.

Experiment Number	Factor 1	Factor 2	Factor 3	Factor 4
1	100 µm	Linear	Flat	20%
2	100 µm	Hexagonal	Edge	40%
3	100 µm	Moroccan star fill	Inclined at 45°	60%
4	200 µm	Linear	Edge	60%
5	200 µm	Hexagonal	Inclined at 45°	20%
6	200 µm	Moroccan star fill	Flat	40%
7	300 µm	Linear	Inclined at 45°	40%
8	300 µm	Hexagonal	Flat	60%
9	300 µm	Moroccan star fill	Edge	20%

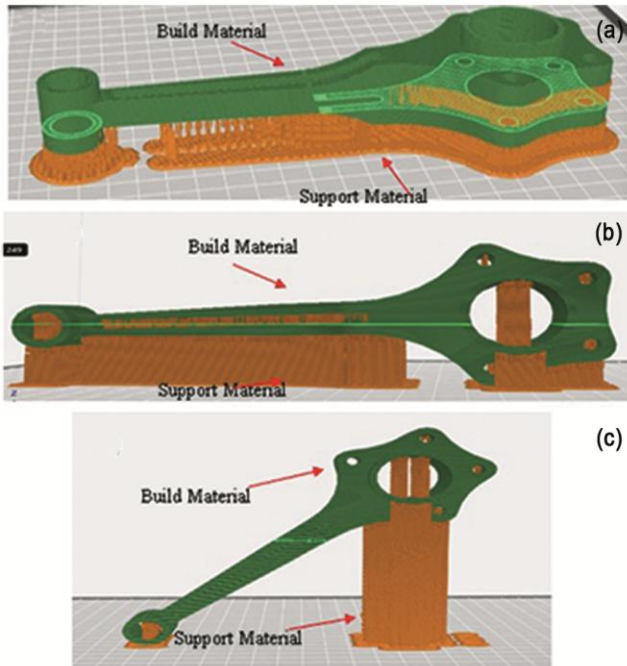


Fig. 3 — Type of infill pattern (a) Linear, (b) Hexagonal and (c) Moroccan star fill.

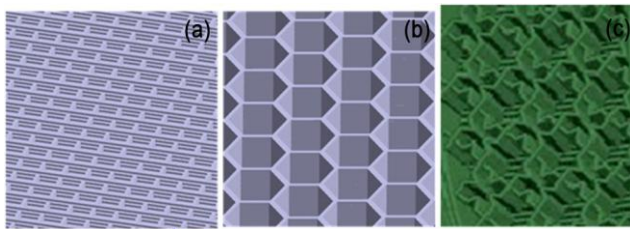


Fig. 4 — Orientation of specimens on FDM platform (a) Flat, (b) Edge and (c) Inclined.

was observed that traditional tools are insufficient to remove the support material.

## 2.2 Measurement

Cylindricity, flatness and dimensional accuracy of FDM manufactured products are very significant aspects, which are considered by researchers. The cylindricity is a three-dimensional tolerance which indicates roundness and straightness both along the entire length of a part. The value of '0' mm cylindricity represents an ideal cylinder case<sup>24</sup>. A perfect flat surface is the one along which all points lie in a single plane. The flatness and cylindricity were evaluated by using the standard ASME Y14.5M-1994<sup>1</sup>. The flat and cylindrical portion selected for the measurement is shown in Fig. 5. In metrology, CMM is being used to automate the process of inspection which has huge increased inspection capabilities. Flatness, cylindricity, radial dimension

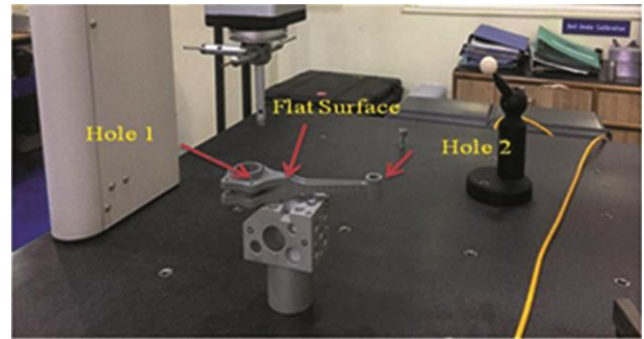


Fig. 5 — Measurement of flatness and cylindricity using CMM.

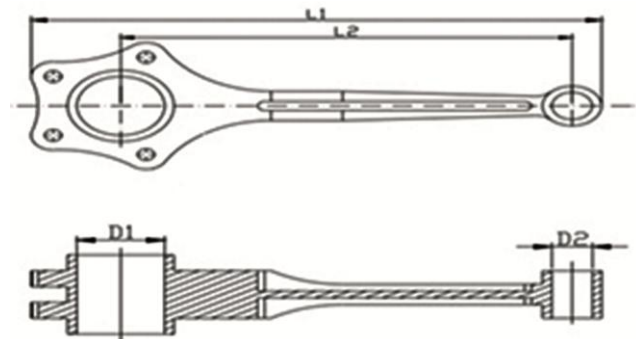


Fig. 6 — Selected linear and radial dimension of the component.

and linear dimension evaluation of automotive components (connecting rod) were performed by using CMM. In this research work, CONTURA G-2 CMM machine was used for the measurement. All axes of this machine are having 4-sided Carl Zeissair bearings for precise measurement. CONTURA G-2 is also equipped with C99 controller. It provides CAA for real-time dynamic correction. Selected linear and radial dimension used for the measurement is highlighted in Fig. 6. CMM has remarkably improved the confidence levels in forecasting of quality at the inspection stage. The software associated with CMM does not directly provide many features like lines, planes, cylinders, circles etc. However, it gives data in the form of cloud points. The measured value of linear dimension, radial dimension, flatness and cylindricity is reported in Table 3.

## 2.3 Statistical Analysis of measured data

Experimental measured data of Table 3, for the linear dimension, radial dimension, flatness and cylindricity was analyzed by using statistical software Minitab 14. The details of the data analysis process are discussed in the next sub-section as below.

### 2.3.1 Signal to Noise (S/N) ratio analysis

To examine the effect of process variables caused by each factor, the S/N ratio was used. It was

observed that the experimental results varied linearly when they were presented in S/N ratios. The quality characteristic ‘smaller is the better’ was considered for the data analysis. S/N ratio ( $\eta$ ) can be obtained by using Eq.(1) (Sood *et al.*<sup>7</sup>).

$$\eta = -10\log(\text{MSD}) \quad \dots (1)$$

$$\text{MSD} = \sigma^2 - (Y_{\text{ave}} - Y_0)^2 \quad \dots (2)$$

where, MSD stands for Mean-Square Deviation,  $\sigma^2$  is the variance,  $Y_0$  is the target value (0 in this design) and  $Y_{\text{ave}}$  is the average value of (n) data points. The value of MSD can be determined by using Eq. 2. For each run of the experiments, the S/N ratio was determined and reported in Table 4. The optimum factor level was selected by using Main effect plot of S/N ratio and reported in Table 5. Significance of individual factor was also calculated by the

comparison of calculated F-value found from experimental data with standard tabulated F-value at 95% CI level. The effect of the individual process parameters can be determined by ANOVA Eqs. 3-6.

$$S_T = (n \eta - \bar{\eta})^2 \quad \dots (3)$$

where, ( $S_T$ ) stands for total sum of square,  $\eta_0$  is the overall mean of (S/N) ratio and n is the total no of experiment<sup>25</sup>.

$$SS_j = \sum_{i=1}^l (\eta_{ji} - \bar{\eta})^2 \quad \dots (4)$$

$$V_j = \frac{SS_j}{f_j} \quad \dots (5)$$

$$F_j = \frac{V_j}{V_e} \quad \dots (6)$$

Table 3 — Measured value of the selected dimension and form error.

Exp. no	CAD Dimension	No of replicate	Linear dimension (mm)		Radial dimension (mm)		Flatness (mm)	Cylindricity (mm)		Building time per component (hr)
			L1	L2	D1	D2	Fy	Cy <sub>1</sub>	Cy <sub>2</sub>	BT
			202.56	160.26	31.20	14.40				
1		3	200.09	159.03	30.64	14.02	0.100	0.08	0.14	11:50
2		3	200.14	159.68	30.61	13.91	0.163	0.06	0.28	17:09
3		3	200.77	159.66	30.61	13.95	0.210	0.09	0.37	25:32
4		3	200.40	159.25	30.75	13.91	0.199	0.18	0.32	08:44
5		3	200.84	159.69	30.71	14.01	0.096	0.16	0.34	08:12
6		3	200.41	158.79	30.66	13.81	0.105	0.13	0.31	10:53
7		3	200.93	159.49	30.64	13.99	0.135	0.33	0.35	05:45
8		3	199.82	159.04	30.52	13.75	0.109	0.16	0.30	05:58
9		3	198.99	159.71	30.50	13.87	0.040	0.19	0.31	06:28

Table 4 — S/N ratio analysis of the measured value.

Exp. No	Average value of flatness (mm)	Average value of cylindricity (mm)	Average % error in linear dimension	Average % error in radial dimension	S/N ratio for flatness	S/N ratio for cylindricity	S/N ratio for linear dimension	S/N for Radial dimension
1	0.100	0.11	0.99	2.22	20.0	19.2	0.09	-6.93
2	0.163	0.17	0.78	2.65	15.8	15.4	2.16	-8.46
3	0.210	0.23	0.63	2.51	13.6	12.8	4.01	-7.99
4	0.199	0.25	0.85	2.42	14.0	12.0	1.41	-7.68
5	0.096	0.25	0.60	2.14	20.4	12.0	4.44	-6.61
6	0.105	0.22	0.99	2.91	19.6	13.2	0.09	-9.28
7	0.135	0.34	0.64	2.32	17.4	9.4	3.88	-7.31
8	0.109	0.23	1.06	3.35	19.3	12.8	-0.51	-10.50
9	0.040	0.25	1.05	2.96	28.0	12.0	-0.42	-9.43

Table 5 — Optimum condition for minimum fatness, cylindricity, dimensional accuracy in the linear and radial direction.

S.N	Shape error	Layer thickness	Infill pattern	Orientation	Infill density	Model value
1	Flatness	300 μm	Moroccan star fill	Flat	20%	0.0158
2	Cylindricity	100 μm	Linear	Flat	20%	0.116
3	Percentage error in linear dimension	100 μm	Hexagonal	Inclined at 45°	40%	0.5935
4	Percentage error in radial dimension	100 μm	Linear	Inclined at 45°	20%	1.749

The higher F-value signifies that the process response is getting affected by the factor. The F-values for the DA, flatness and cylindricity for this study was reported in Tables 6-9 , respectively. The main effect plot of signal to noise ratio for DA, flatness and cylindricity are shown in Fig. 7 (a-d).

**2.3.2 Development of empirical model for the flatness and cylindricity**

Empirical model was derived by using least square multi variable linear regression analysis. The response function Y for the DA, flatness and cylindricity in terms of four input process parameters (X<sub>1</sub>, X<sub>2</sub>, X<sub>3</sub> and X<sub>4</sub>) can be expressed by Eq. 7.

$$Y = f(X_1, X_2, X_3, X_4) \quad \dots (7)$$

The linear Eq. for the experimental data can be defined by Eqs. 8-13.

$$Y = \beta_0 + \beta_1 \times X_1 + \beta_2 \times X_2 + \beta_3 \times X_3 + \beta_4 \times X_4 \quad \dots (8)$$

$$\sum_{i=1}^n Y_i = n\beta_0 + \sum_{i=1}^n \beta_1 \times X_{1i} + \sum_{i=1}^n \beta_2 \times X_{2i} + \sum_{i=1}^n \beta_3 \times X_{3i} + \sum_{i=1}^n \beta_4 \times X_{4i} \quad \dots (9)$$

$$\sum_{i=1}^n Y_i \times X_1 = \sum_{i=1}^n \beta_0 \times X_1 + \sum_{i=1}^n \beta_1 \times X_1^2 + \sum_{i=1}^n \beta_2 \times X_1 \times X_2 + \sum_{i=1}^n \beta_3 \times X_1 \times X_3 + \sum_{i=1}^n \beta_4 \times X_1 \times X_4 \quad \dots (10)$$

$$\sum_{i=1}^n Y_i \times X_2 = \sum_{i=1}^n \beta_0 \times X_2 + \sum_{i=1}^n \beta_1 \times X_1 \times X_2 + \sum_{i=1}^n \beta_2 \times X_2^2 + \sum_{i=1}^n \beta_3 \times X_2 \times X_3 + \sum_{i=1}^n \beta_4 \times X_2 \times X_4 \quad \dots (11)$$

$$\sum_{i=1}^n Y_i \times X_3 = \sum_{i=1}^n \beta_0 \times X_3 + \sum_{i=1}^n \beta_1 \times X_1 \times X_3 + \sum_{i=1}^n \beta_2 \times X_2 \times X_3 + \sum_{i=1}^n \beta_3 \times X_3^2 + \sum_{i=1}^n \beta_4 \times X_3 \times X_4 \quad \dots (12)$$

$$\sum_{i=1}^n Y_i \times X_4 = \sum_{i=1}^n \beta_0 \times X_4 + \sum_{i=1}^n \beta_1 \times X_1 \times X_4 + \sum_{i=1}^n \beta_2 \times X_2 \times X_4 + \sum_{i=1}^n \beta_3 \times X_3 \times X_4 + \sum_{i=1}^n \beta_4 \times X_4^2 \quad \dots (13)$$

where, (n) is the total no of experiment and β<sub>0</sub>, β<sub>1</sub>, β<sub>2</sub>, β<sub>3</sub> & β<sub>4</sub> are the regression coefficient. Y<sub>i</sub> is the output response and X<sub>1</sub>, X<sub>2</sub>, X<sub>3</sub> and X<sub>4</sub> are the input parameters. The value of unknown coefficient of the regression Eq. (8) can be determined by using Eqs (9-13). In this study the output parameters were flatness, cylindricity, percentage error in linear dimension and percentage error in radial dimension, and input parameters were layer thickness, infill pattern, orientation and infill density. The obtained regression equation for the flatness (F<sub>y</sub>) cylindricity (C<sub>y</sub>), percentage error in linear dimension (% ΔL) and percentage error in radial dimension (%ΔR) are as shown in Eqs (14- 17).

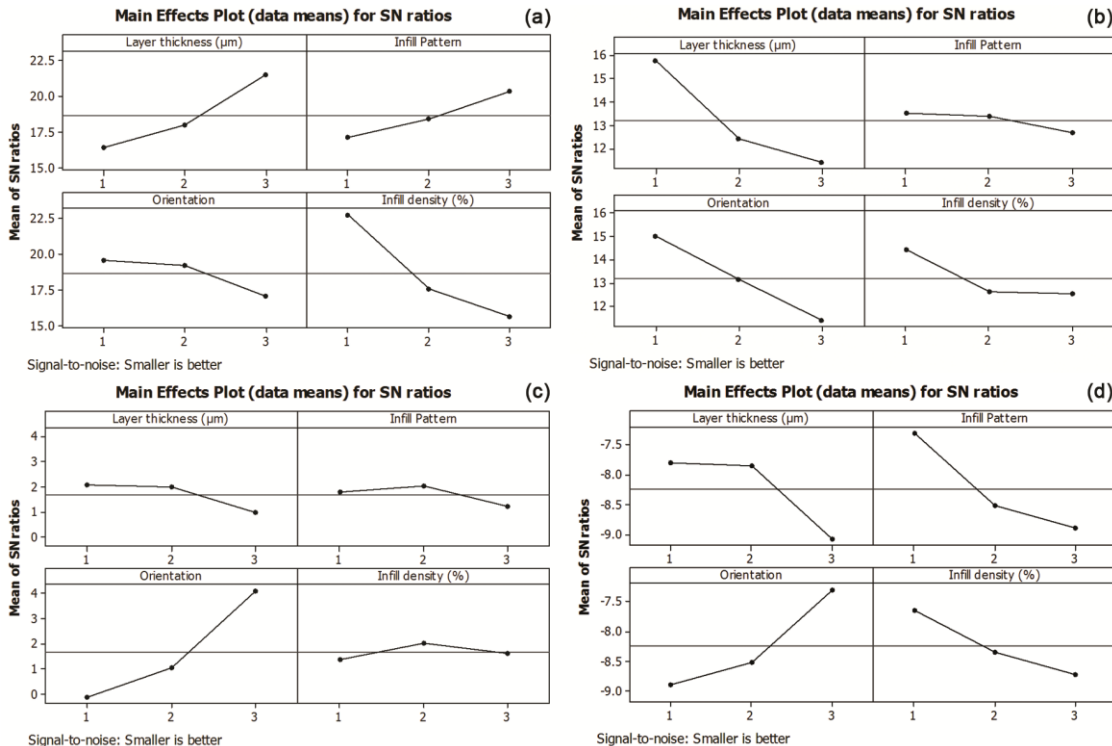


Fig. 7 — Main effect plot of SN ratio (a) Flatness, (b) Cylindricity, (c) Percentage error in linear dimension and (d) Percentage change in radial dimension.



$$F_y = 0.816 - 0.000315X_1 - 0.01317X_2 + 0.02117X_3 + 0.002350X_4 \quad \dots (14)$$

$$C_y = 0.0044 + 0.000517X_1 + 0.0000X_2 + 0.0433X_3 + 0.000833X_4 \quad \dots (15)$$

$$\% \Delta L = 1.09 + 0.000583X_1 + 0.0317X_2 - 0.195X_3 - 0.00083X_4 \quad \dots (16)$$

$$\% \Delta R = 1.90 + 0.00208X_1 + 0.237X_2 - 0.252X_3 + 0.00800X_4 \quad \dots (17)$$

where,  $X_1$  is the layer thickness ( $\mu\text{m}$ ),  $X_2$  is the infill pattern (1 for linear, 2 for hexagonal and 3 for moroccan star fill),  $X_3$  is the orientation (1 for flat, 2 along edge and 3 for inclined at  $45^\circ$ ) and  $X_4$  is the infill density (%). The above developed empirical model predicts the DA, flatness and cylindricity for the any combination of process parameters within the experimental domain. F test was carried out for checking the goodness of fit for the model.

### 3 Results Summary and Discussion

Table 3 shows the measured value of dimensional accuracy, flatness and cylindricity. In this research work percentage error in linear dimension ( $\% \Delta L$ ), percentage error in radial dimension ( $\% \Delta R$ ), flatness ( $F_y$ ) and cylindricity ( $C_y$ ) has been evaluated. Results of measurement depicted that actual dimensions of the fabricated components were smaller than CAD dimension due to shrinkage of material during solidification. Figure 7 shows the main effect plots of the S/N ratio for the DA, flatness and cylindricity. A regression model was developed for the forecasting of

DA, flatness and cylindricity in terms of input process parameters. These regression models were tested for checking adequacy and fitness by the analysis of variance (ANOVA). The P-value (probability value) of the suggested regression models were less than 0.05 and F-value of regression models were greater than tabulated F-value in the confidence interval of 95%. The correlation coefficient ( $R^2$ ) decides the fitting accuracy of the regression models. Typically higher value of  $R^2$  (close to 1.0), indicate better fit of regression model for the response variables. In the above model, value of ( $R^2$ ) was 0.976 for flatness Eq.14, 0.9234 for the cylindricity Eq. 15, 0.906 for percentage error in linear dimension Eq. 16, and 0.893 for the percentage error in radial dimension Eq.17. It indicates that there was a strong co-relation between actual and predicated value. Tables 6 shows the ANOVA of response variable cylindricity. Table 7 shows the ANOVA of response factor flatness. Table 8 and Table 9 show the ANOVA value of response factors percentage error in linear dimension and percentage error in radial dimension respectively. Higher value of percentage contribution indicates more significant process parameters on output response. From Table 6 it can be concluded that percentage contribution of orientation was high for cylindricity.

#### 3.1 Effect of process parameters

##### 3.1.1 Layer thickness

Layer thickness has significant effect on the dimensional accuracy and cylindricity. Figure 7a shows that the value of flatness is minimum at layer

Table 6 — ANOVA table for the cylindricity.

Source	DF	Seq SS	Seq MS	F-Value	P-Value	% Contribution	Remarks
Regression	4	0.028950	0.007238	12.03	0.017		$F_{0.025,4,4} = 9.6045$
Layer Thickness	1	0.016017	0.016017	26.63	0.007	51.08	
Infill Pattern	1	0.000000	0.000000	0.00	1.000	0.00	$F > F_{0.025,4,4}$
Orientation	1	0.011267	0.011267	18.73	0.012	35.93	Model is adequate
Infill density	1	0.001667	0.001667	2.77	0.171	5.32	
Error	4	0.002406	0.000601			7.67	
Total	8	0.031356					

Table 7 — ANOVA table for the flatness.

Source	DF	Seq SS	Seq MS	F-Value	P-Value	%Contribution	Remarks
Regression	4	0.022936	0.005734	42.29	0.002		$F_{0.025,4,4} = 9.6045$
Layer Thickness	1	0.005954	0.005954	43.91	0.003	25.36	
Infill Pattern	1	0.001040	0.001040	7.67	0.050	4.43	$F > F_{0.025,4,4}$
Orientation	1	0.002688	0.002688	19.82	0.011	11.45	Model is adequate
Infill density	1	0.013254	0.013254	97.75	0.001	56.45	
Error	4	0.000542	0.000136			2.31	
Total	8	0.023478					

Table 8 — ANOVA table for the percentage error in linear dimension.

Source	DF	Seq SS	Seq MS	F-Value	P-Value	% Contribution	Remarks
Regression	4	0.256250	0.064063	9.65	0.025		$F_{0.025,4,4} = 9.6045$
Layer Thickness	1	0.020417	0.020417	3.08	0.154	7.22	
Infill Pattern	1	0.006017	0.006017	0.91	0.395	2.13	
Orientation	1	0.228150	0.228150	34.37	0.004	80.68	$F > F_{0.025,4,4}$
Infill density	1	0.001667	0.001667	0.25	0.643	0.59	Model is adequate
Error	4	0.026550	0.006638			9.39	
Total	8	0.282800					

Table 9 — ANOVA table for the percentage error in radial dimension.

Source	DF	Seq SS	Seq MS	F-Value	P-Value	% Contribution	Remarks
Regression	4	1.1301	0.28253	8.38	0.032		$F_{0.05,4,4} =$
Layer Thickness	1	0.2604	0.26042	7.73	0.050	20.59	6.3882
Infill Pattern	1	0.3361	0.33607	9.97	0.034	26.57	
Orientation	1	0.3800	0.38002	11.28	0.028	30.04	$F > F_{0.05,4,4}$
Infill density	1	0.1536	0.15360	4.56	0.100	12.14	Model is adequate
Error	4	0.1348	0.03370			10.66	
Total	8	1.2649					

thickness 300  $\mu\text{m}$ . According to Wu *et al.*<sup>26</sup> at 300  $\mu\text{m}$ , FDM component have maximum mechanical properties. As tensile strength of the component increases, the value of flatness automatically decreases. Figures 7 (b and d) show that the dimensional accuracy and cylindricity is better at the smaller layer thickness of 100  $\mu\text{m}$ . Dimensional error in radial direction and cylindricity is produced due to the triangulation of the circular geometry. Lower thickness has less triangulation error, which results better cylindricity. Figure 7c shows that layer thickness is insignificant process parameters for the dimensional error in linear dimension. From Table 3 it can be concluded that FDM process parameters have significant effect on the building time of the component. The building time was found to be minimum corresponding to process parameter i.e. layer thickness 300  $\mu\text{m}$ , flat orientation, infill density 20 % and hexagonal infill pattern.

### 3.1.2 Infill pattern

Infill pattern play a major role in the mechanical properties and porosity in the FDM component. Hexagonal pattern have the maximum tensile strength (Aljohani and Desai<sup>18</sup>). However, it was observed that infill patterns were not the significant process parameters for the flatness and dimensional error in linear dimension. Figure 7a shows that the moroccan star fill pattern has lowest value of flatness. Figures 7 (b and d) illustrate that linear pattern have the lowest cylindricity and dimensional error in radial dimension. It was observed that infill pattern have significant effect on dimensional error in radial direction.

### 3.1.3 Orientation

Figures 7 (a and b) show that flat surface have the lowest value of the flatness and cylindricity. Figures 7(c and d) show that dimensional accuracy of the fabricated component is better along 45° orientation. It was observed that orientation has significant effect on linear as well as radial dimension of the fabricated component.

### 3.1.4 Infill density

The effect of infill density is very high for the flatness. Figures 7(a, b and d) show that at 20% infill density dimensional accuracy in radial dimension and forms error in fabricated PLA component were minimum. Figure 7(c) shows that infill density was the insignificant process parameter for the response factor dimensional accuracy in linear dimension.

## 4 Optimization of Process Parameters

The overall performance analysis of any machine is evaluated on the basis of the number of output response. Table 5 shows that optimum condition for DA, flatness and cylindricity were different. Hence it was required to find out the best process parameter condition, which optimizes DA, flatness and cylindricity. So multi objective optimization technique was required. In this work, utility theory was employed for the optimization.

Utility theory is a powerful tool used for the multi objective optimization of the decision variables. This theory converts multiple response factors into a single objective function. It is presumes that a decision was taken to maximize the utilization of the utility (Jayadithya *et al.*<sup>27</sup>). According to utility theory, the



mathematical expression of joint utility is expressed below:

$$U(Z_1, Z_2, Z_3, Z_4) = f(U_1(Z_1), U_2(Z_2), U_3(Z_3) \dots \dots \dots U_n(Z_n)) \dots (18)$$

Where,  $U_i(Z_i)$  are the utility of the  $i^{th}$  attribute. The sum of individual utility makes the overall utility function. For an independent attribute, the utility function is given below:

$$U(Z_1, Z_2, Z_3 \dots \dots \dots Z_n) = \sum_{i=1}^n U_i(Z_i) \dots (19)$$

The overall utility in terms of weight function can be expressed as:

$$U(Z_1, Z_2, Z_3 \dots \dots \dots Z_n) = \sum_{i=1}^n W_i \times U_i(Z_i) \dots (20)$$

where,  $W_i$  is the weight function. Logarithmic scale is used for the evaluating the performance scale.

$$P_i = A \times \log_{10} \left( \frac{Z_i}{Z_1} \right) \dots (21)$$

where,  $Z_i$  is the value of quality characteristics of  $i^{th}$  attribute,  $A$  is the constant and ' $Z_1$ ' is the minimum acceptable value. The value of constant term can be evaluated with the help of optimal condition.

If  $Z_i = Z^*$  (where  $Z^*$  is the optimal value) and ( $P_i=9$ ) for this case.

$$P_i = A \times \log_{10} \left( \frac{Z_i}{Z^*} \right) \dots (22)$$

The overall utility value can be calculated as:

$$U = \sum_{i=1}^n W_i \times P_i \dots (23)$$

The overall utility value can be used as a single objection function. Optimization is carried out by using the 'larger is the better' quality characteristics.

**4.1 Construction of performance scale.**

• **Flatness**

$Z^* = 0.0158$ mm optimum value of flatness (refer Table 7).

$Z_1 = 0.21$ mm minimum acceptable value of flatness (refer Table 3).

$$A = -8.01$$

$$P_{Fy} = -8.01 \times \log_{10} \left( \frac{Z_{Fy}}{0.21} \right) \dots (24)$$

• **Cylindricity**

$Z^* = 0.158$ mm optimum value of cylindricity (refer Table 7).

$Z_1 = 0.34$ mm minimum acceptable value of cylindricity (refer Table 4).

$$A = -27.25$$

$$P_{Cy} = -27.25 \times \log_{10} \left( \frac{Z_{Cy}}{0.21} \right) \dots (25)$$

• **Percentage error in Linear dimension**

$Z^* = 0.5935\%$  optimum value of percentage error in Linear dimension (refer Table 7).

$Z_1 = 1.06\%$  minimum acceptable value of percentage error in Linear dimension (refer Table 3).

$$A = -35.73$$

$$P_{el} = -35.73 \times \log_{10} \left( \frac{Z_{el}}{1.06} \right) \dots (26)$$

• **Percentage error in Radial dimension**

$Z^* = 1.749 \%$  optimum value of percentage error in radial dimension (refer Table 7).

$Z_1 = 3.35\%$  minimum acceptable value of percentage error in radial dimension (refer Table 3).

$$A = -31.88$$

$$P_{er} = -31.88 \times \log_{10} \left( \frac{Z_{er}}{3.35} \right) \dots (27)$$

**4.2 Utility value calculation**

The utility value of each group of experiment was calculated by using the Eq. 28. In this work equal weight function (1/4) was used for evaluating overall utility value. Table 10 shows the summery of utility value and S/N ratio corresponding to the overall utility value. The quality characteristics 'larger is the better' is implied for the evaluation of S/N ratio. Mini Tab 14 was used for evaluation of S/N ratio and main effect plot of S/N ratio. Figure 8 shows the best conditions of the selected process parameters for DA, flatness and cylindricity.

$$U = P_{Fy} \times W_{Fy} + P_{Cy} \times W_{Cy} + P_{el} \times W_{el} + P_{er} \times W_{er} \dots (28)$$

**4.3 Confirmation test**

A confirmation test was conducted corresponding to the best process parameters condition. The best

Table 10 — Utility value and S/N ratio.

Exp. No.	U <sub>Fy</sub>	U <sub>Cy</sub>	U <sub>el</sub>	U <sub>ed</sub>	U <sub>overall</sub>	S/N ratio
1	2.58	13.4	1.05	5.69	5.68	15.1
2	0.88	8.20	4.75	3.24	4.27	12.6
3	0	4.62	8.07	7.24	4.98	13.9
4	0.18	3.63	3.42	4.50	2.93	9.3
5	2.72	3.63	8.83	6.20	5.35	14.6
6	2.41	5.15	1.06	1.94	2.64	8.4
7	1.53	0	7.83	5.08	3.61	11.2
8	2.28	4.62	0	0	1.73	4.8
9	5.76	3.63	0.14	1.73	2.82	9.0

Table 11 — Best value of process parameters for flatness and cylindricity.

S.N	Shape Error	Layer Thickness	Infill Pattern	Orientation	Infill density	Calculated From Model	Experimental Value
1	Flatness (mm)					0.147 ± 0.0173	0.154 mm
2	Cylindricity (mm)			Inclined at		0.185 ± 0.0366	0.212 mm
3	Percentage error in linear dimension	100 µm	Linear	45°	20 %	0.5935 ± 0.121	0.649 %
4	Percentage error in radial dimension					1.749 ± 0.122	1.683 %

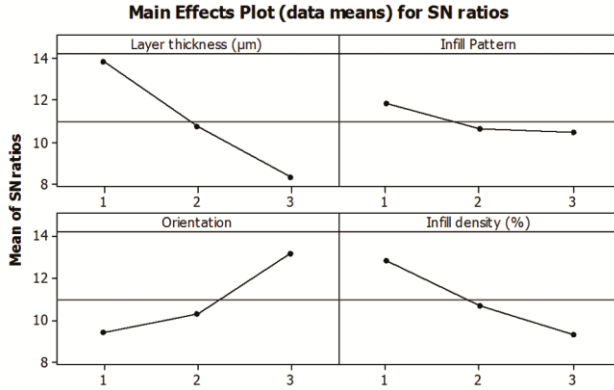


Fig. 8 — Main effect plot of S/N ratio of optimum solution.

value of process parameters were layer thickness (100 µm), infill pattern (linear), orientation (inclined at 45°) and infill density (20 %). Owing to uncertainty of the output response, three component corresponding the best process parameter condition were fabricated and average value of DA, flatness and cylindricity were reported in Table 11. Due to uncertainty output response was expected to fall in the range of the confidence interval (CI)<sup>4</sup>. The value of DA, flatness and cylindricity can be evaluated by using Eq. 29. Results of the conformation test depict that the suggested models for the DA, flatness and cylindricity were adequate in the 95% of CI within the experimental domain.

$$\left. \begin{aligned}
 \text{Expected Cylindricity} &= (C_{y_{opt}} \pm C.I) \\
 \text{Expected Flatness} &= (F_{y_{opt}} \pm CI) \\
 \text{Expected \% error in linear dimension} &= (\% \Delta L \pm CI) \\
 \text{Expected \% error in radial dimension} &= (\% \Delta R \pm CI)
 \end{aligned} \right\} \dots(29)$$

**5 Calculation of IT Grade**

ISO standard UNIEN 20286-I (16901) was used for the calculation of international tolerance grade (IT grade)<sup>28</sup>. Eq. 30 was used for the computation of fundamental tolerance ‘i’ and Eq. 31 was used for the calculation of tolerance unit<sup>29</sup>

$$i = 0.45 \sqrt[3]{D} + 0.001D \dots(30)$$

Table 12 — IT grade for the linear and radial dimension.

Exp. No	L1	Deviation in linear dimension (mm)	n	IT grade	D1	Deviation in radial dimension	n	IT grade
1	200.09	2.47	853.2	IT14	30.64	0.56	358.7	IT13
2	200.14	2.42	835.9	IT14	30.61	0.59	378.0	IT13
3	200.77	1.79	618.3	IT13	30.61	0.59	378.0	IT13
4	200.40	2.16	746.1	IT14	30.75	0.45	288.3	IT13
5	200.84	1.72	594.1	IT13	30.71	0.49	313.9	IT13
6	200.41	2.15	742.7	IT14	30.66	0.54	345.9	IT13
7	200.93	1.63	563.0	IT13	30.64	0.56	358.7	IT13
8	199.82	2.74	946.5	IT14	30.52	0.68	435.6	IT14
9	198.99	3.57	1233.2	IT15	30.50	0.7	448.4	IT14

$$n = \left( \frac{|D_n - D_m|}{i} \right) \dots(31)$$

Where D is the geometric mean range of nominal size and D<sub>m</sub> is the measured value and ‘n’ is the tolerance unit. For present, radial dimension (D<sub>r</sub> = 32.2 mm) and study linear dimension (L<sub>1</sub> = 202.56 mm) were used for determination of IT grades. Table 12 shows the value of IT grades of radial and linear dimension. The results showed that radial dimension have greater IT grade as compared to linear dimension. It leads to conclude that components fabricated through MakerBot printer have more dimensional errors in radial dimension than that of linear dimension.

**6 Conclusions**

The main objective of present work was to find out the impact of process variables viz., layer thickness, infill pattern, orientation and infill density on DA, flatness and cylindricity of FDM parts. Experiments were designed by using Taguchi orthogonal array L<sub>9</sub>. A regression model was established to predict the DA, flatness and cylindricity. Following conclusion can be drawn from this study.

- (i) The build orientation, layer thickness and infill density were the most influencing process variables in FDM process. However infill pattern has less significance on the flatness.
- (ii) From the (S/N) analysis for the flatness it was found that layer thickness 300 µm, Infill Pattern

(Moroccan Star fill), Orientation (flat) and Infill density (20%) were the optimal process parameters.

- (iii) The optimum conditions of process parameters for cylindricity were layer thickness (100  $\mu\text{m}$ ), Infill Pattern (linear), orientation (flat) and infill density (20 %).
- (iv) The empirical model developed for the DA, flatness and cylindricity was adequate in the range of 95% confidence interval within the experimental domain.
- (v) The optimum conditions of the process parameters for DA, flatness and cylindricity were different. Multi objective optimization (utility theory) was employed to find out the best process parameters condition.
- (vi) The best condition for the DA, flatness and cylindricity were layer thickness (100  $\mu\text{m}$ ), infill pattern (linear), orientation (inclined at 45°) and density (20 %).
- (vii) This work was limited to commonly used material PLA only. In future, presented methodology may be applied for the other material also.

## Reference

- 1 Senthilkumaran K, Pandey P M & Rao P V M, *Rapid Prototyp J*, 18 (2012) 38.
- 2 Keo C C & Su S J, *Indian J Eng Mater Sci*, 20 (2013) 465.
- 3 Keo C C & Shi Z S, *Indian J Eng Mater Sci*, 19 (2012) 157.
- 4 Jain P K, Pandey P M & Rao P M V, *Virtual Phys Prototyp*, 3 (2008) 177.
- 5 Melenka G W, Schofield, Jonathon S, Dawson, Jonathon R & Carey J P, *Rapid Prototyp J*, 21 (2016) 618.
- 6 Narang R & Chhabra D, *IJFRCSE*, 3 (2017) 41.
- 7 Paul R & Paul S, *J Manuf Syst*, 36 (2015) 231.
- 8 Mohamed O A, Sood S H M & Bhowmik J L, *Rapid Prototyp J*, 23 (2016) 736.
- 9 Sood A K, Ohdar R K, & Mahapatra S S, *Mater Des*, 30 (2009) 4243.
- 10 Relvas C, Ramos A N, Completo A N & Simoes J A, *Proc Inst Mech Eng*, 22 (2012) 2023.
- 11 Brajlilh T, Valentan B, Balic J & Drstvensek I, *Rapid Prototyp. J*, 17( 2011)64.
- 12 Chang D Y & Chang B H, *Int J Adv Manuf Technol*, 53 (2011)1027.
- 13 Das P, Chandran R, Chandran R & Anand S, *Procedia Manuf*, 1 (2015) 343.
- 14 Saqib S & Urbanic J, *An Experimental Study to Determine Geometric and Dimensional Accuracy Impact Factors for Fused Deposition Modelled Parts*, 4<sup>th</sup> International Conference on Changeable, Agile, Reconfigurable and Virtual Production (CARV2011), Montreal, Canada 2011
- 15 Urbanic O A, Urbanic S H & Bhowmik J L, *Appl Math*, 4 (2016) 10052.
- 16 Nithin S T D, Sivadasan M & Singh N K, *Mater Today*, 5 (2018)1327.
- 17 Das P, Mhapsekar K, Sushmit C, Samant R & Anand S, *Comput Aided Des Appl*, 14 (2017) 1.
- 18 Aljohani A & Desai S, *Am J Eng Appl Sci*, 11 (2018)1076.
- 19 Knoop F, *SFF Symp*, (2017) 2757.
- 20 Juneja M, Thakur N, Kumar D, Gupta A, Bajwa B & Jindal P, *Addit Manuf*, 22 (2018) 243.
- 21 Kozior T & Kundera C Z, *Procedia Eng*, 192 (2017) 463.
- 22 Kozior T, Dopke C, Grimmelsmann N, Junger I J & Ehrmann A, *Adv Mech Eng*, 10 (2018) 1.
- 23 Maurya N K, Rastogi V & Singh P, *Evergreen Joint J Novel Carbon Res Sci Green Asia Strategy*, 6 (2019) 207.
- 24 Maurya NK, Rastogi V & Singh P, *I2M*, 18(2019)353.
- 25 Mahmood S, Qureshi A J & Nazarbayev D T, *Addit Manuf*, 21 (2018) 183.
- 26 Wu W, Geng P, Li G, Zhao D, Zhang H, Zhao J, *Mater*, 8 (2015) 5834.
- 27 Jayadithya R, Deekshith B, Chaithnya P L & Rajyalakshmi G, *Int J Sci Appl Inform Technol*, 3 (2014) 1.
- 28 Singh J, Singh R & Singh H, *Prog Addit Manuf*, 2 (2017)85.
- 29 Singh R, *J Mech Sci Technol*, 25 (2011) 1011.